Intermolecular Dimerization within Pillared, Layered Clay Templates

Gary P. Wiederrecht,* Giselle Sandi, Kathleen A. Carrado, and Sönke Seifert

Chemistry Division, Argonne National Laboratory, Argonne, Illinois 60439

Received March 26, 2001. Revised Manuscript Received August 8, 2001

Solutions of pyrene in the presence of a pillared, layered montmorillonite clay produce hybrid organic−inorganic materials with substantial molecular loading in the gallery regions between the clay layers. The results are in sharp contrast to other aromatics, such as benzene, naphthalene, or perylene, which show minimal incorporation of the molecules into the gallery regions of the clay. We present evidence that the unusual affinity for pyrene to form intermolecular dimers is the reason for the high loading. Pyrene monomers are easily introduced to the layers. Through steric hindrance, subsequent intermolecular dimer formation is allowed, and they are captured by the pillared, layered structure. CW and time-resolved emission spectra strongly indicate the presence of face-to-face intermolecular dimers (excimers) within the clay galleries. The combination of the ease of high molecular loading into an inorganic, high aspect ratio template and the collective optical properties of the organic layer may be useful as a new means to create hybrid structures.

Introduction

Inorganic crystalline solids that function as templates for assembling organic molecular films can produce new hybrid materials with unusual electronic, catalytic, or structural characteristics.[1−7] However, self-assembly of these hybrid structures is frequently difficult, and it is usually critical that the organic molecules be incorporated at high density to induce collective structural and/or electronic properties in the organic layers. In this vein, we have explored the large molecule-dependent variations in the degree of organic molecular loading in a pillared interlayered clay (PILC) template derived from montmorillonite.[7,8] The PILC consists of sheets of an aluminosilicate structure shown in Figure 1a, with Al_2O_3 pillars that maintain an interlamellar spacing on the order of 10 Å (Figure 1b,c).[7] Pyrolysis of organics intercalated into the interlamellar regions of the PILC has been shown to produce new forms of porous carbon for use as anode electrodes.[7,8] For developing porous carbon with this technique, we have determined that pyrene incorporates into the gallery (interlamellar) region of PILCs at more than an order of magnitude higher concentration (5−6 wt %) relative to other aromatics such as benzene,[9] naphthalene, or perylene. Given that these molecules bracket the size of pyrene, spatial or steric hindrance of pyrene monomers is not the reason for the high pyrene concentration.

The high incorporation of pyrene into the gallery region of PILC is fortuitous, because the photophysical properties of pyrene are extremely well-studied and known to be highly sensitive to the local environment.[10−20] More specifically, the relative peak intensities and energies of the emission profile of pyrene change dramatically in different environments. These changes are particularly noticeable when on the surfaces of highly polar clay surfaces.[17,21] Pyrene also has a high affinity for forming intermolecular dimers (excimers) with red-shifted and structureless emission profiles, both in solution and on clays.[11,22,23]

In this study, X-ray scattering and optical spectroscopies are used as probes of the hybrid pyrene/PILC

(1) Lidzey, D. G.; Bradley, D. D. C.; Virgili, T.; Armitage, A.; Skolnick, M. S.; Walker, S. *Phys. Rev. Lett.* **1999**, *82*, 3316−19.
(2) Braun, M.; Tuffentsammer, W.; Wachtel, H.; Wolf, H. C. *Chem. Phys. Lett.* **1999**, *303*, 157−164.
(3) Kagan, C. R.; Mitzi, D. B.; Dimitrakopoulos, C. D. *Science* **1999**, *286*, 945−47.
(4) Wang, J.; Merino, J.; Aranda, P.; Galvan, J.-C.; Ruiz-Hitzky, E. *J. Mater. Chem.* **1999**, *9*, 161−7.
(5) Ijdo, W. L.; Pinnavaia, T. J. *Chem. Mater.* **1999**, *11*, 3227−31.
(6) Winkler, B.; Dai, L.; Mau, A. W.-H. *J. Mater. Sci. Lett.* **1999**, *18*, 1539−41.
(7) Sandi, G.; Thiyagarajan, P.; Carrado, K. A.; Winans, R. E. *Chem. Mater.* **1999**, *11*, 235−40.
(8) Sandi, G.; Winans, R. E.; Carrado, K. A. *J. Electrochem. Soc.* **1996**, *143*, L95-L98.
(9) Winans, R. E.; Carrado, K. A. *J. Power Sources* **1995**, *54*, 11−15.
(10) Kalyanasundaram, K.; Thomas, J. K. *J. Am. Chem. Soc.* **1977**, *99*, 2039−2044.
(11) Dellaguardia, R. A.; Thomas, J. K. *J. Phys. Chem.* **1984**, *88*, 964−970.
(12) Matsui, K.; Usuki, N. *Bull. Chem. Soc. Jpn.* **1990**, *63*, 3516−3520.
(13) Zilberstein, J.; Bromberg, A.; Berkovic, G. *J. Photochem. Photobiol. A* **1994**, *77*, 69−81.
(14) Udachin, K. A.; Ripmeester, J. A. *J. Am. Chem. Soc.* **1998**, *120*, 1080−1081.
(15) Ogawa, M.; Aono, T.; Kuroda, K.; Kato, C. *Langmuir* **1993**, *9*, 1529−33.
(16) Ogawa, M.; Wada, T.; Kuroda, K. *Langmuir* **1995**, *11*, 4598−4600.
(17) Kuykendall, V.; Thomas, J. K. *Langmuir* **1990**, *6*, 1346−1350.
(18) Tahani, A.; Karroua, M.; Damme, H. V.; Levitz, P.; Bergaya, F. *J. Colloid. Interface Sci.* **1999**, *216*, 242−249.
(19) Suib, S. L.; Kostapapas, A. *J. Am. Chem. Soc.* **1984**, *106*, 7705−7710.
(20) Cione, A. P. P.; Scaiano, J. C.; Neumann, M. G.; Gessner, F. *J. Photochem. Photobiol. A* **1998**, *118*, 205−9.
(21) Liu, X.; Thomas, J. K. *Langmuir* **1991**, *7*, 2808−2816.
(22) Liu, X.; Thomas, J. K. *Chem. Mater.* **1994**, *6*, 2303−08.
(23) Liu, X.; Iu, K.-K.; Thomas, J. K. *J. Phys. Chem.* **1989**, *93*, 4120−4128.

10.1021/cm010262f CCC: $20.00
Published on Web 10/05/2001

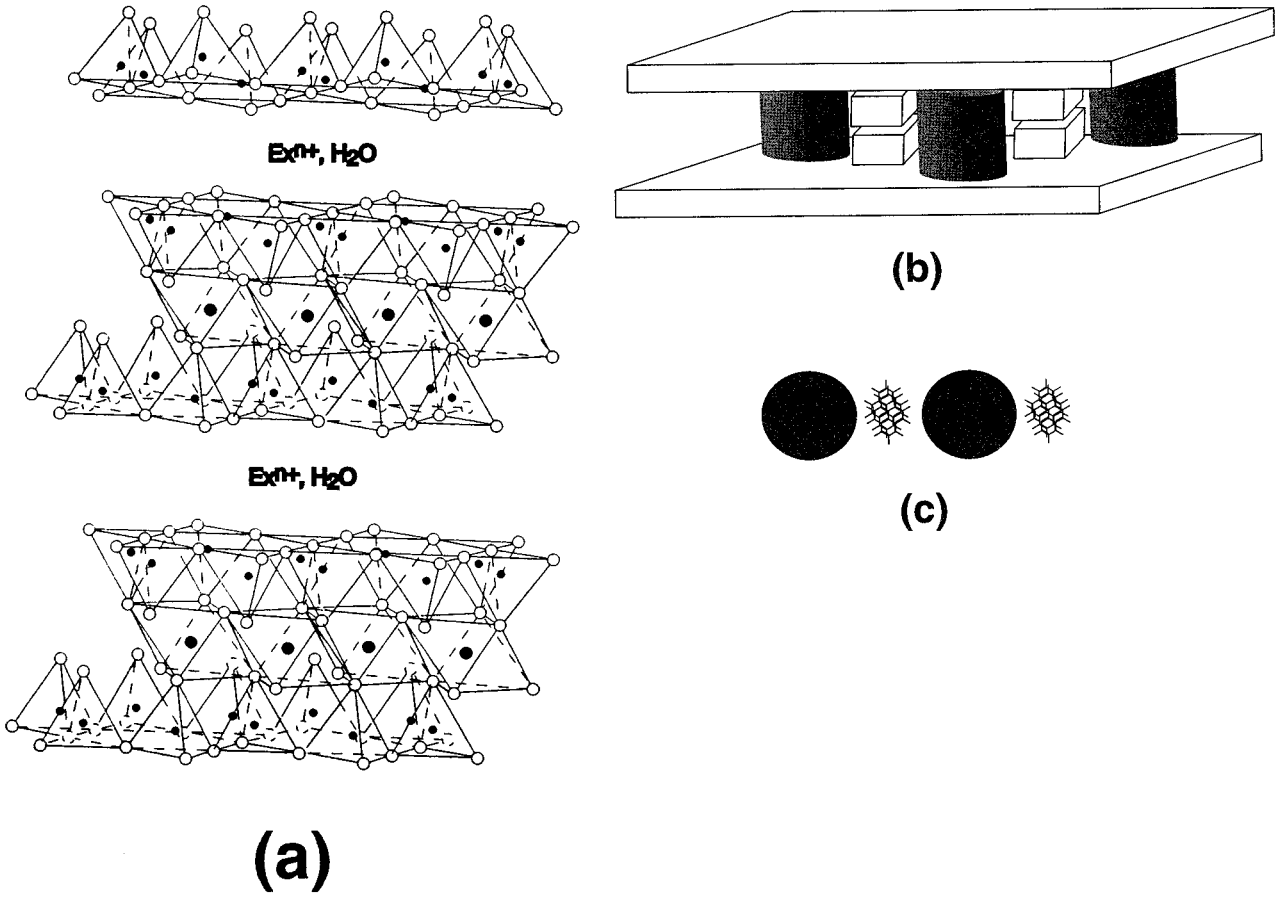

Figure 1. The layered structure of montmorillonite is shown (a), along with side view (b) and edge view (c) schematics of the pyrene incorporation into the PILC as dimers. Solid cylinders (b) and circles (c) are the Al_2O_3 pillars.

material. By monitoring the excimer emission, we report strong evidence that the reason for the high incorporation of pyrene is the formation of intermolecular dimers in the gallery regions of the PILC. Through steric hindrance, the dimers (excimers) are trapped at greater efficiency within the layers, producing an easily prepared organic−inorganic layered hybrid material. We also show that the initiation of organic loading in PILCs by pyrene dimers further explains the observation of organic bilayers in the gallery regions of PILCs as determined by the molecular H/C ratio and ^{13}C NMR.[24]

Experimental Section

The PILC was synthesized according to procedures given previously.[7−9] The PILC was loaded at room temperature by stirring the pillared clay in a 0.02 M solution of pyrene in toluene at room temperature overnight, producing dark green samples. The samples were repeatedly washed with toluene to remove pyrene from solution, thus ensuring that the optical spectra were associated only with pyrene that is loaded into the PILC. PILCs are generally preactivated at 400 °C to convert the initial oxyhydroxy aluminum species to rigid Al_2O_3 spacers. This results in a two-dimensional microporous network of molecular dimensions (8 × 8)−(10 × 10) Å depending upon the properties of the particular clay.[25−27] This permits the incorporation of pyrene and the other control aromatic molecules (benzene, naphthalene, perylene). For example, the van der Waals dimensions of a pyrene molecule are 11.6 × 8.8 × 3.5 Å.[27] The width is adequate for pyrene incorporation into a PILC such as from beidellite clay, where windows of 10 × 10 × 7.5 Å were estimated.[27] We assume that the windows of our PILC are similar in size. Thermal analysis measurements with a TA Instruments TGA−DTA (model number SDT2960) verified the pyrene loading to be 5−6 wt %. This degree of loading was also previously observed for a pillared beidellite clay.[27] The green color is a result of the acid catalysis by the alumina pillars in the PILC, similar to what happens in a Friedel−Crafts arylation or Schöll reaction:[28]

$$2ArH \xrightarrow[H^+]{AlCl_3} Ar-Ar + H_2$$

This can produce a network of aromatic rings, as discussed by Lewis.[29] Often a change in color upon organic loading in clays can be attributed to radical cations stabilized by iron ion impurities, but the iron has been removed from this particular clay by the commercial supplier, to a final loading of only 0.7 wt % Fe_2O_3. Attempts to load the PILC with the control molecules benzene, naphthalene, or perylene did not produce colored samples. Optical or thermal gravimetric analysis indicated that there was less than 1% organic loading of these control molecules.

Additional clay templates were used as controls to clarify the nature of pyrene within PILC. These were different treatments of the starting material (unpillared) clay, a Ca^{2+}-montmorillonite (mt) called Bentolite L. One control was

(24) Winans, R. E.; Sandi, G.; Carrado, K.; Thiyagarajan, P. Structure of Carbons Prepared with Pillared Clay Templates; 23rd Biennial Conference on Carbon, 1997, Pennsylvania State University.
(25) Occelli, M. L.; Drake, B.; Gould, S. A. C. *J. Catal.* **1993**, *142*, 337−348.
(26) Tsaio, C.-J.; Carrado, K. A.; Botto, R. E. *Microporous Mesoporous Mater.* **1998**, *21*, 45−51.
(27) Plee, D.; Gatineau, L.; Fripiat, J. J. *Clays Clay Miner.* **1987**, *35*, 81−88.
(28) Balaban, A.; Nenitzescu, T. In *Friedel−Crafts Chemistry*; Olah, G., Ed.; Wiley: New York, 1973; Vol. 2.
(29) Lewis, I. C. *Carbon* **1980**, *18*, 191.

heated (calcined) for 4 h at 400 °C in order to completely collapse the inorganic layers (no gallery spacing) and one was an untreated mt that possessed an interlamellar gap of ~5.5 Å due to hydrated Ca^{2+} ions.

A time-correlated single photon counting (TCSPC) spectrometer was used to determine the emission time constants and spectral characteristics of pyrene in mt. The experimental setup consists of a Ti:sapphire laser that is acousto-optically cavity-dumped at 800 kHz. Home-built RF electronics are used to control the phase of the acoustic wave relative to the optical pulse within the oscillator. This phase matching technique permits nearly 70% of the pulse energy to be cavity-dumped, resulting in up to 50 nJ/pulse at 800 nm.[30,31] The output is frequency-doubled to 400 nm, producing an average excitation irradiance of 0.5 W/cm^2 (peak irradiance of 4×10^7 W/cm^2). A Hamamatsu R3809U multichannel plate photomultiplier in conjunction with an EG&G 9308 time analyzer and 9307 discriminators permit a time resolution of 50 ps. Three-dimensional spectral data was obtained by stepping the detection monochromator and obtaining a kinetic scan at each wavelength, corrected by throughput through the monochromator and sensitivity of the multichannel plate at different wavelengths. The results are compared to CW emission spectra taken on a Princeton Instruments spectrophotometer. The emission spectra were obtained with an excitation wavelength of 397 nm by stirring a washed, 2 mg pyrene/clay sample in toluene in a 1 cm quartz cuvette.

Small-angle X-ray scattering (SAXS) experiments were performed at the Basic Energy Sciences Synchrotron Radiation Center at the Advanced Photon Source (APS) using slurries of the pyrene/clay samples in 1.5 mm quartz capillaries. Slurries, rather than dry samples, were used for the SAXS experiments so that any swelling of the clays under the conditions present when the hybrid system is being prepared could be identified. SAXS is preferable to X-ray diffraction (XRD) for wet samples, especially such dilute slurries as these. Furthermore, the APS data permits SAXS measurements down to 0.002 Å^{-1}, permitting the observation of all physically reasonable swelling possibilities for the clay samples in toluene. The results were compared to the XRD of powder samples to further corroborate any swelling of the clays in liquids.

Results and Discussion

The SAXS results on all three pyrene prepared samples (PILC, calcined mt, uncalcined mt) while in toluene are shown in Figure 2a, while the XRD results on dry powders are shown in Figure 2b. The peaks provide the *d* spacings for the clays, which is the sum of the clay layer (9.6 Å) and the interlamellar gap (gallery). In the toluene solvent, the results indicate a 10.6 Å gallery in PILC and 7.1 Å for uncalcined mt. The XRD results on dry powders indicate an 8.9 Å gallery in PILC and 5.3 Å for uncalcined mt. Thus, swelling of the gallery regions in the PILC and uncalcined mt by 1−2 Å is observed in solution relative to XRD.[7−9] The data further confirm that, even in solution, the gallery remains collapsed for the calcined mt (note the lack of a significant *d* spacing peak in the SAXS of Figure 2a). No scattering signal was observed below *Q* values of 0.20 Å^{-1} (not shown), proving that larger interlamellar distances do not exist.

The CW emission spectra of pyrene in the PILC and the two mts are shown in Figure 3. The pyrene/PILC sample shows a broad emission band at 490 nm and

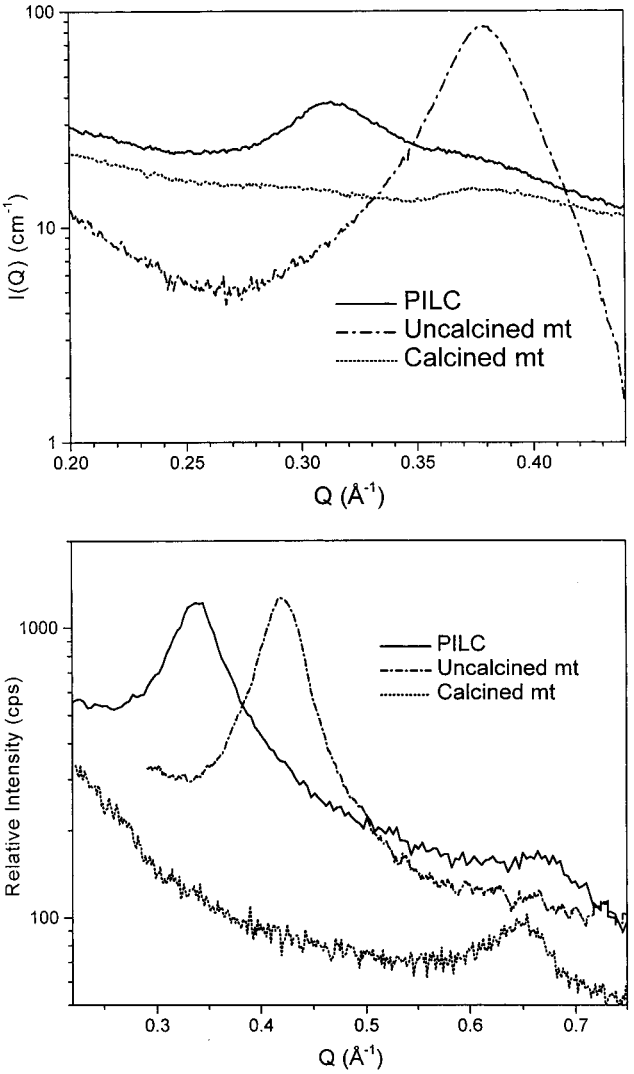

Figure 2. (a) X-ray scattering and (b) X-ray diffraction spectra for pyrene-loaded clay samples in toluene performed at the Advanced Photon Source. Swelling of the gallery regions in the PILC and uncalcined mt by 1−2 Å is observed in solution relative to X-ray diffraction from dry clay samples. The calcined mt remains collapsed in both environments. The *x*-axis scale in part b is provided in *Q* for comparison purposes to part a and corresponds to 3−12° 2θ.

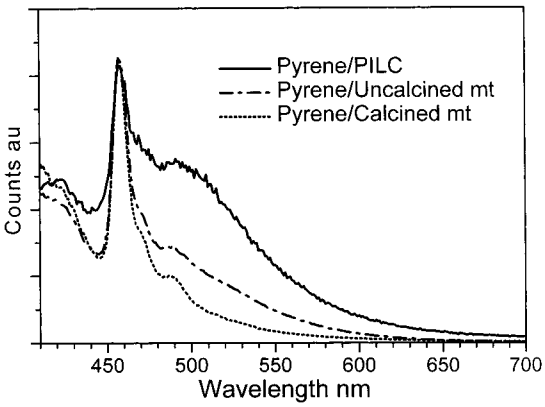

Figure 3. The CW emission scans of pyrene incorporated into the PILC and mts are shown for excitation at 397 nm. Only the PILC sample shows significant amounts of pyrene excimer emission at 500 nm.

is assigned to the excimer emission band of pyrene. The face-to-face excimer has an intermolecular gap of

(30) Ramaswamy, M.; Ulman, M.; Paye, J.; Fujimoto, J. G. *Opt. Lett.* **1993**, *18*, 572−74.
(31) Pshenichnikov, M. S.; Boeij, W. P. d.; Wiersma, D. A. *Opt. Lett.* **1994**, *19*, 572−4.

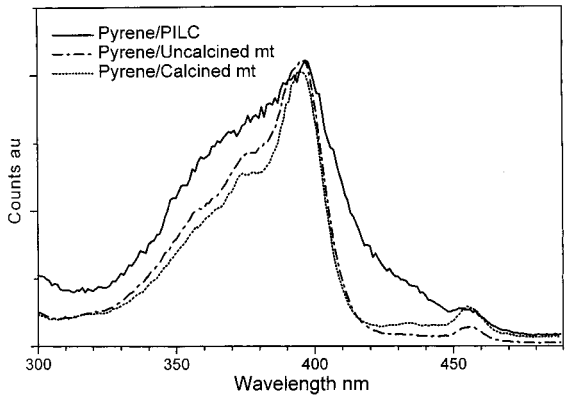

Figure 4. The CW excitation profiles of pyrene incorporated into the PILC and mts are shown for excitation at 397 nm. The red-shifted components of the PILC sample indicate the presence of ground-state dimers in the PILC.

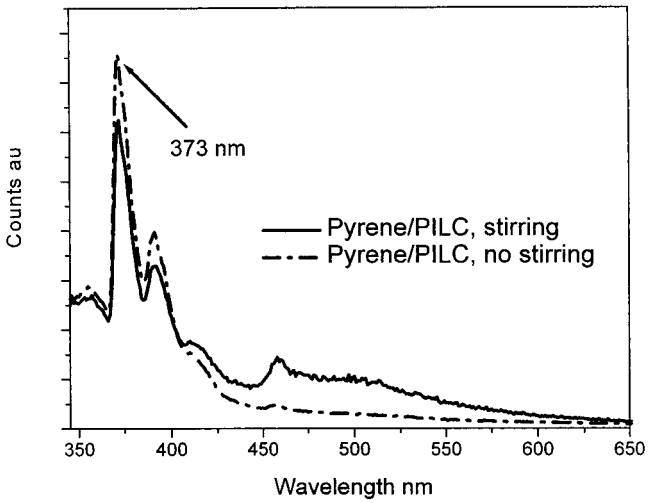

Figure 5. Fluorescence from pyrene/PILC in toluene while stirring or not stirring at an excitation wavelength of 338 nm. The stirred sample favors the larger particles containing more lamellar regions vs outer surfaces. The larger excimer emission vs monomer emission in the stirred sample indicates that the excimers are present in the gallery regions of the PILC.

3.34 Å,[32] permitting formation in the interlamellar regions of the PILC. While the excimeric emission is shifted from the 470 nm value typically seen in solution, the red shift is consistent with previously observed pyrene excimers in highly polar environments.[21] The signal magnitude from the excimer band is strongly reduced in the uncalcined mt and is nonexistent in the collapsed, calcined mt. This result indicates that the excimer emission originates predominantly from within the layers of the clays. The weak excimer emission in the uncalcined mt results from some incorporation of intermolecular pyrene dimers in the gallery regions, though largely excluded due to the presence of water. Emission studies of the excimer in PILC were also performed under N_2 and in air, with only a 5% quenching of the emission in air. Since the presence of O_2 has been shown to efficiently quench pyrene excimer emission,[22] the excimers are presumed to be largely present in the interlamellar regions, where exposure to O_2 is limited.

Figure 4 illustrates the excitation spectra for pyrene in the PILC and the two mts, with monitoring at 500 nm near the peak of the excimeric emission from pyrene in the PILC. The pyrene in PILC shows significantly red shifted components, consistent with the presence of pyrene dimers.[22] The excitation bands also gradually broaden and become structureless, with the progression calcined mt < uncalcined mt < PILC. This is likely a combination of the delocalization of the electronic excitations due to the presence of ground-state dimers and also the heterogeneous environment of the PILCs, with the pillars being more polar than the clay itself. The location of the pyrene dimer relative to the pillar will determine the local polarity of the environment and alter the excitation profile. The bands in the excitation and emission scans at 457 nm are assigned to pyrene cations, known to exist on the surfaces of clays.[21]

Figure 5 further illustrates that the structureless emission is largely from pyrene excimers that lie within the layers, i.e., not on the clay particle surfaces. Here the emission from pyrene in PILC is monitored with an excitation wavelength of 338 nm, centered on the lowest energy absorption band pyrene. The predominance of the 373 nm emission band has been previously observed when pyrene monomer lies on the polar surface of clays or zeolites.[22] Data are shown for samples that are either stirred or not stirred. In the case for the unstirred sample, only the smallest clay particles with larger surface-to-layer ratios remain in the path of the excitation beam, while the larger particles drop out of the excitation beam. The data show that the dimeric excimer signal drops when the sample is not stirred, while the monomeric signal increases. This shows that the dimeric excimer emission signal originates from within the layers in larger clay particles, while the monomeric signal is present in greater quantities on the surface of the clay in the smaller, higher surface to volume clay particles.

The data above indicate that the reason for the unusually high loading into the gallery regions of PILC is that pyrene, once incorporated into the interlamellar region, forms ground state dimers and becomes sterically too hindered to easily exit the clay. This also explains the conundrum that naphthalene loads less well into the clay despite its smaller size, as naphthalene does not form dimers as well as pyrene.[32] Benzene and perylene also are not known to form intermolecular dimers as readily as pyrene.[32] It is interesting that the covalent networking of pyrene in PILCs does not dramatically alter the electronic structure of the intermolecular dimer, indicating that the networked structure is likely formed after the face-to-face dimers are formed. This again supports our conclusion that formation of intermolecular dimers is a critical step that occurs first in order to induce steric hindrance, providing enough time to allow for the networking reaction to proceed. It should be noted that pyrene dimers have been shown to form readily in many different media,[23,33,34] though the use of the intermolecular dimerization as a vehicle to higher molecular loadings in

(32) Birks, J. B. *Photophysics of aromatic molecules*; Wiley: London, 1970.

(33) Yamazaki, T.; Tamai, N.; Yamazaki, I. *Chem. Phys. Lett.* **1986**, *124*, 326−29.

(34) Fujii, T.; Shimizu, E.; Suzuki, S. *J. Chem. Soc., Faraday Trans.* **1988**, *84*, 4387−4395.

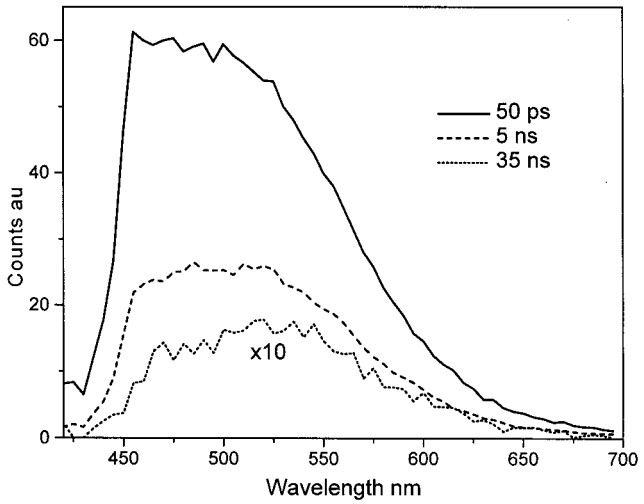

Figure 6. The time-resolved emission spectra for pyrene in the PILC at different time delays are shown. The presence of the excimer emission within the time resolution of the instrument indicates that the pyrene dimers are already present in a face-to-face geometry and are not formed through diffusion.

organic/inorganic templates has not been reported to our knowledge.

The high loading initiated by pyrene dimer formation also helps explain reports that the network of aromatic rings in pyrene loaded PILCs is actually a bilayer.[24] This conclusion was reached due to two measurements. First, the low molecular H/C ratio of 0.04 in the pyrolized organic following removal of the PILC suggests that the molecules near the pillars are not terminated with hydrogen.[8] Second, ^{13}C NMR on the samples shows that only sp^2 carbons exist, so that aromaticity is preserved near the pillars. This leaves a scenario such as that of nanotubes, whereby capping or bending is achieved with a combination of aromatic pentagons and heptagons. These data suggests that a bilayer in the gallery exists that is capped at the pillars with a curved structure.

Figure 6 shows time-resolved single photon counting (TCSPC) spectra at 50 ps, 5 ns, and 35 ns for pyrene in the PILC. The most important aspect is that the excimer is formed within the time resolution of the instrument (50 ps), indicating that the excimer formation is the result of pyrene dimers in close face-to-face proximity.[11] Longer times scales on the order of nanoseconds would indicate diffusion of monomers to form excimers and are not observed here. Figure 7 illustrates the kinetics of the excimer emission decay in the high (450 nm) and low (575 nm) energy regions of the emission spectrum. The two kinetic profiles show a large difference in the decay rates and cannot be fit to single exponential decays. The lack of first-order decay kinetics illustrates that the pyrene excimer is present in a highly heterogeneous environment. The lower energy excimers in the more polar regions of the gallery have longer lifetimes than the higher energy excimers in the low-polarity regions. To eliminate the possibility that excited-state interactions or exciton annihilation is influencing these results, we decreased the amount of pyrene loaded by a factor of 20 and 150. No change in the spectral or kinetic emission characteristics was observed.

The kinetic profiles fit well to previous models of pyrene excimers in heterogeneous environments, modeled by a Gaussian distribution of excimer energies:[22,35]

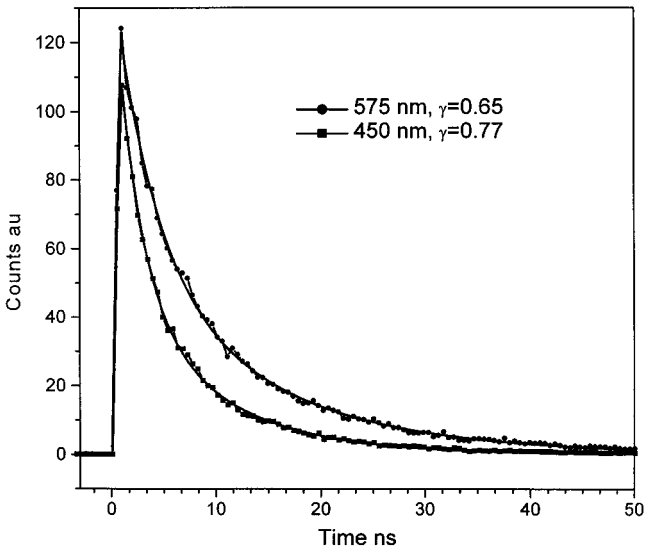

Figure 7. The decay kinetics for the pyrene dimer in the PILC at 450 and 575 nm is shown. The nonexponential decays and wide variation in decay times indicate a heterogeneous environment for the dimers in the gallery regions of the PILC.

$$\frac{I(t)}{I(0)} = \frac{\int_{-\infty}^{\infty} \exp(x^2)\, \exp[-kt\, \exp(\gamma x)]\mathrm{d}x}{\int_{-\infty}^{\infty} \exp(-x^2)\mathrm{d}x} \qquad (1)$$

where γ is measure of the Gaussian distribution, k is the rate constant of excimer decay, $I(t)$ is the intensity of emission as a function of time, and $I(0)$ is the initial emission intensity. The data fits shown in Figure 7 use values of $\gamma = 0.77$ and $\tau = 9.0$ ns at 450 nm. At 575 nm, values of $\gamma = 0.65$ and $\tau = 13.7$ ns are obtained. These values for γ and τ are similar to those observed on the surface of mordenite clay and zeolites.[22] It is interesting that the lower energy excimers probed at 575 nm, likely an indication that they are present in the higher polarity regions near the pillars, have a lower value of γ. This suggests that the packing is better near the pillars, consistent with the view that the network of aromatic rings begins near the pillars due to acid catalysis, and limits large differences in the alignment of isolated excimers relative to the clay layers.

Conclusions

We have presented transient optical and X-ray scattering data for pyrene-loaded PILCs. The data provide evidence for the efficient formation of face-to-face intermolecular pyrene dimers in the gallery regions of pillared clay templates. The formation of the dimers is a likely reason for the increased loading (5−6 wt %), due to steric hindrance in the galleries upon dimer formation. A variety of control experiments using clays that cannot incorporate dimers due to spatial constraints and other aromatics that do not easily form intermolecular dimers support the presence of face-to-face interlamellar pyrene dimers. The initiation of the loading process with the creation of face-to-face dimers also justifies the observation of organic bilayers in the gallery region. The combination of the ease of high

(35) Albery, W. J.; Bartlett, P. N.; Wilde, C. P.; Darwent, J. R. *J. Am. Chem. Soc.* **1985**, *107*, 1854−58.

molecular loading through dimerization into an inorganic template and modified optical emission properties of the organic layer may be useful for creating new hybrid optical materials.

Acknowledgment. This work was supported by the Division of Chemical Sciences, Office of Basic Energy Sciences, U.S. Department of Energy, under contract number W-31-109-ENG-38 and benefited from the use of the Basic Energy Sciences Synchrotron Radiation Center at the Advanced Photon Source at Argonne National Laboratory.

CM010262F